Available online at www.sciencedirect.com
SCIENCE DIRECT
Geochimica et Cosmochimica Acta 70 (2006) 1603–1615
Geochimica
www.elsevier.com/locate/gca

Boron isotopic composition of atmospheric precipitations and liquid–vapour fractionations

E.F. Rose-Koga [a,b,*], S.M.F. Sheppard [a], M. Chaussidon [c], J. Carignan [c]

[a] *Ecole Normale Supérieure de Lyon, CNRS UMR 5570, Laboratoire de Science de la Terre, 46 allée d'Italie, 69364 Lyon cedex 07, France*
[b] *Woods Hole Oceanographic Institution, Department of Geology and Geophysics, Woods Hole, MA 02543, USA*
[c] *Centre de Recherches Pétrographiques et Géochimiques, 15 rue Notre Dame des Pauvres, 54501 Vandoeuvre-les-Nancy, France*

Received 11 July 2005; accepted in revised form 5 January 2006

Abstract

Boron isotope compositions ($\delta^{11}B$) and B concentrations of rains and snows were studied in order to characterize the sources and fractionation processes during the boron atmospheric cycle. The $^{11}B/^{10}B$ ratios of instantaneous and cumulative rains and snows from coastal and continental sites show a large range of variations, from -1.5 ± 0.4 to $+26.0 \pm 0.5$‰ and from -10.2 ± 0.5 to $+34.4 \pm 0.2$‰, respectively. Boron concentrations in rains and snows vary between 0.1 and 3.0 ppb. All these precipitation samples are enriched in ^{10}B compared to the ocean value ($\delta^{11}B = +39.5$‰). An empirical rain-vapour isotopic fractionation of +31‰ is estimated from three largely independent methods. The deduced seawater–vapour fractionation is +25.5‰, with the difference between the rain and seawater fractionations principally reflecting changes in the speciation of boron in the liquid with ~100% $B(OH)_3$ present in precipitations. A boron meteoric water line, $\delta D = 2.6\delta^{11}B - 133$, is proposed which describes the relationship between δD and $\delta^{11}B$ in many, but not all, precipitations. Boron isotopic compositions of precipitations can be related to that of the seawater reservoir by the seawater–vapour fractionation and one or more of (1) the rain-vapour isotopic fractionation, (2) evolution of the $\delta^{11}B$ value of the atmospheric vapour reservoir via condensation–precipitation processes (Rayleigh distillation process), (3) any contribution of vapour from the evaporation of seawater aerosols, and (4) any contribution from particulate matter, principally sea salt, continental dust and, perhaps more regionally, anthropogenic sources (burning of biomass and fossil fuels). From the $\delta^{11}B$ values of continental precipitations, a sea salt contribution cannot be more than a percent or so of the total B in precipitation over these areas.

1. Introduction

Boron is a quite variable trace constituent in the atmosphere with concentrations usually between 0.2 and 300 ppb (e.g., Fogg and Duce, 1985; Duce, 1996; Miyata et al., 2000; Rose et al., 2000a). It is present in both gaseous and particulate forms with the former probably representing more than 90–95% of the total (Fogg and Duce, 1985). Principal sources are usually considered to be (1) for gaseous boron: evaporation of sea water, both directly and indirectly via sea water aerosol evaporation, and volcanic emissions, and (2) for particulate boron: salts from evaporated sea water aerosols, volcanic and terrestrial dusts. As suggested by the systematics of the B, Cl and Na contents of epiphytic lichens which average atmospheric precipitations over periods of a few months to a few years, the variations of the B contents and B/Na ratios of precipitation reflect a selective scavenging of particulate B relative to gaseous B (Rose et al., 2000a). The lichen data also indicate that the atmospheric residence time of gaseous B is ~16 times that of particulate B in agreement with previous estimates (obtained from rain data) which are of 19–36 days and of 2–6 days for gaseous and particulate B, respectively (Fogg and Duce, 1985). Gaseous and particulate anthropogenic contributions may be locally or regionally important.

* Corresponding author. Present address: Laboratoire Magmas et Volcans, CNRS UMR 6524 5, Rue Kessler, 63038 Clermont-Ferrand cedex, France. Fax: +33 0 4 73 34 67 44.
E-mail address: e.koga@opgc.univ-bpclermont.fr (E.F. Rose-Koga).

0016-7037/$ - see front matter © 2006 Elsevier Inc. All rights reserved.
doi:10.1016/j.gca.2006.01.003

Rain and snow are considered to be the major agents scavenging boron from the atmosphere, although gas exchange with the oceans has also been proposed. A quantitative understanding of boron in the atmosphere, however, does not yet exist: in particular the atmospheric evolution of seawater derived B remains enigmatic.

The boron isotopic ratios, $^{11}B/^{10}B$, of the major reservoirs—sea water, continental crust, volcanic emissions—that are potentially related to processes influencing atmospheric boron, are often quite different (e.g., Palmer and Swihart, 1996). Thus, study of the isotope geochemistry of boron should improve our understanding of the processes that control or influence atmospheric boron and this part of the boron cycle.

The boron concentration and $\delta^{11}B$ value ($\delta^{11}B$ in ‰ is defined as $[(^{11}B/^{10}B)_{sample}/(^{11}B/^{10}B)_{standard}) - 1] \times 1000$ of the oceans are uniform at approximately 4500 ppb and +39.5‰ (relative to SRM 951), respectively (e.g., Schwarcz et al., 1969; Palmer et al., 1987; Spivack and Edmond, 1987). Though the major terrestrial B reservoir is the continental crust (~70% of the terrestrial boron budget), the oceans represent the major B reservoir in the hydrologic cycle since the atmosphere contains approximately 3×10^4 times less B than seawater. Extremely large B isotopic fractionations are observed in the hydrologic cycle relative to the $\delta^{11}B$ value of average continental crust (−10‰, Chaussidon and Albarède, 1992). However, the continental crust is also quite variable isotopically with $\delta^{11}B$ values between ~−30 and ~+30‰ (e.g., Palmer and Swihart, 1996). Large B isotopic variations are observed for riverine dissolved B, from ~−5% to ~+50% (Lemarchand et al., 2000; Rose et al., 2000b), these variations reflecting both the isotopic heterogeneity of the crust and the isotopic fractionations taking place during erosion processes. Although a few data on fumarolic condensates of hydrothermal and volcanic systems exist (overall $\delta^{11}B$ ranges from −9.3 to +21.4‰; Kanzaki et al., 1979; Nomura et al., 1982; Palmer and Sturchio, 1990), data on the concentration and $^{11}B/^{10}B$ ratio of atmospheric boron (i.e., gas) are extremely scarce. Boron concentrations range from 13.8 to 248 ppb (64% of the [B] <72 ppb) and $\delta^{11}B$ values between −13.6 and +5.1‰ (Miyata et al., 2000). Data available for rain and snow show concentrations ranging from 0.2 to 385 ppb and $\delta^{11}B$ values from −12.8 to +45‰ (Fogg and Duce, 1985; Spivack, 1986; Xiao et al., 1992; Eisenhut and Heumann, 1997; Miyata et al., 2000; Chetelat et al., 2005). The concentration ratio of atmospheric gaseous B to dissolved rain B in a given region can be estimated from data in Fogg and Duce (1985) and Miyata et al. (2000): for two oceanic islands and a coastal station the ratios range from 10 to 20, and for a continental station in Colorado it is 2.

Because boron is nearly always bonded to oxygen in the hydrosphere and lithosphere, its isotope geochemistry is principally controlled by its relative partitioning between trigonal molecules, such as $B(OH)_3$, which tend to concentrate the heavier isotope, ^{11}B, and tetrahedral molecules, such as $B(OH)_4^-$, which tend to concentrate the lighter isotope, ^{10}B. The speciation of boron in natural waters is quite sensitive to pH. Normal seawater contains about 59% of $B(OH)_3$ and 41% of $B(OH)_4^-$ (acidity constant of 8.6 at 20 °C for a salinity of 35‰, recalculated using Kotaka, 1973; Kakihana et al., 1977; Michard, 1989). $B(OH)_3$ and $B(OH)_4^-$ are the dominant species at pHs of <~7.5 and >~9.5, respectively. However, the speciation of boron in the atmosphere is not well characterized.

Interpretation of the relationships among the several potential reservoirs requires knowledge of the relevant chemical and isotopic fractionation factors. The isotopic fractionation factor between two phases A and B is defined as $\alpha_{A-B} = (^{11}B/^{10}B)_A/(^{11}B/^{10}B)_B$, with $1000 \ln \alpha_{A-B} \approx \delta^{11}B_A - \delta^{11}B_B = \Delta_{A-B}$ (this approximation is good within 0.5‰). The availability of such data is quite uneven, especially for B isotope fractionations. Preliminary experimental (Spivack et al., 1990) and empirical (Leeman et al., 1992) data for liquid (brine)-vapour isotope fractionations gave values from ~0 to −3‰ as temperature decreases from 450 to ~150 °C, with the vapour enriched in ^{11}B. At surface temperature, seawater evaporation was studied experimentally by Xiao et al. (2001) by using an air-flow system. For experiments without any bubble bursting, they measured B isotope fractionations between seawater and vapour of +9.8 and +15.6‰ at 25° and 35 °C respectively, with the vapour depleted in ^{11}B, and boron concentrations of 6.2 and 4.4 ppb, respectively. A quite different view of B isotopic fractionation during seawater evaporation was proposed by Chetelat et al. (2005) from closed system experiments in which condensates were produced from seawater evaporation at 60 °C. The fact that the condensates were found to have $\delta^{11}B$ values (from +40.6‰ to +46.5‰) slightly higher than that of seawater (+39.5‰) was taken as an argument showing that $\Delta_{vapour-seawater}$ was slightly positive. Note however that in such an experiment the B isotopic composition of the condensate is the result of at least two isotopic fractionations, one taking place during evaporation at 60 °C and the other one during condensation at an unspecified temperature, so that the exact values of these two isotopic fractionations are difficult to infer precisely.

The goals of the present study are to characterize the processes and the B sources responsible for boron isotopic variations in the atmosphere. Liquid/vapour boron isotopic fractionation factors $\alpha_{liq-vap}$ are inferred based on (1) atmospheric gas and precipitation data, (2) the chemical and isotopic analyses of precipitations (rain and snow), and (3) boron and hydrogen isotope analyses of selected precipitations from coastal and inland environments, including equatorial regions where the evaporation of seawater into the atmosphere principally occurs.

2. Sampling

Rain and snow samples were collected from urban and non-urban areas, at various distances from the ocean

(0–800 km) and at various altitudes (0–4107 m), on two different continents (North America and Asia). Two rain samples were collected on the seashore near San Francisco, California during a single storm event, in order to get a sample at the ocean–continent interface. There are two types of precipitation samples: instantaneous (during an event) and cumulative, over variable durations. Because of its averaging characteristics, the second category can be compared to the information given by lichens, which were previously studied for their B contents (Rose et al., 2000a).

All samples after collection were kept in pre-cleaned Teflon bottles and stored at 4 °C after filtration at 0.45 μm. No sample was acidified, except in the case of snow packs (NE Canada) into which a small amount of distilled nitric acid was added (Simonetti et al., 2000a,b). Both acidified and non-acidified samples were tested for contamination and none was detected. Replicate boron concentration analyses by ICP-MS and ion chromatography after several months of storage yielded reproducible results (standard deviation of 0.1 ppb at most), showing the stability of the sample solutions (Rose et al., 2000a).

Single rain or snow events were sampled in Nepal between 1993 and 1997, using an inert plastic funnel and a Teflon bottle pre-cleaned with the rain or melt water itself. Whenever possible, most of the rain event was sampled. Composite events ($n = 6$) representing in total more than 2 months of rainfall during the 1997 monsoon were also sampled in Katmandu (Nepal). In this latter case, the collector used to collect the integrated rains was exposed to both wet and dry deposition. However, dry deposition was scarce during the monsoon period (Galy, 1999). The chemistry (major cations, anions and O, H and Sr isotopes) of these water samples are reported elsewhere (Rose, 1999; Galy et al., 1999).

During the 1994 winter, snow packs were sampled along a north-south transect in the boreal forest of Québec, between Hudson Bay and Montréal. These samples represent an integration of 2–3 months of precipitation (Simonetti et al., 2000a). Precipitation samples (snow, freezing rain and rain), representing either single or integrated events, were collected during the 1998 winter at a meteorological station close to Montréal (LAS samples). The collectors were opened only when it started raining/snowing (Simonetti et al., 2000b). The chemistry (major cations, trace elements; Pb and Sr isotopes) and the detailed sampling procedures of these samples have been reported by Simonetti et al. (2000a,b).

3. Analytical techniques

3.1. Concentration measurements

Major elements and B concentrations were made at CRPG (France) using well established techniques—ICP-MS Perkin-Elmer ELAN 6000, ion chromatography Dionex 4500i (e.g., Rose et al., 2000a). For B measurements, the eluent was a solution of mannitol 0.1 M with an ICE-AS1 column. Analytical precision (1σ) is better than ±5% for cations, ±10% for anions and ±4% for B concentrations >1 ppb. B concentrations lower than 1 ppb were determined by ICP-MS with a ±6% (1σ) precision.

3.2. Isotopic compositions

B isotopic compositions of 6 natural precipitation waters were measured by ion microprobe (Cameca 3f) at CRPG (France) and the 26 other natural precipitations were measured by ion microprobe (Cameca 1270) at Woods Hole Oceanographic Institution (USA). We followed the procedures for determining the B isotopic composition of river waters described in a previous study (Rose et al., 2000b). Several droplets of rainwater were dried with an infrared lamp on a pure silicon wafer. Care was taken never to exceed 60 °C with the lamp nor let the deposit over dry, once the last liquid was evaporated. Isotopic test on residues for the evaporation of B were carried out on standard solutions, with B concentrations overlapping our range of natural waters, and demonstrated to be negligible (see Fig. 2 in Rose et al., 2000b). During the course of this study, seawater was taken as our reference solution, and repeated $\delta^{11}B$ measurements on the 3f ion probe using the above technique yielded $+39.8 \pm 0.7‰$ (1σ; 11 replicates), and $+39.6 \pm 1.0‰$ (1σ; 5 replicates) on the 1270 ion probe.

On the 3f ion probe, the dried solid residues were sputtered with a 10 kV O^- primary beam, and the 4.5 kV positive secondary $^{10}B^+$ and $^{11}B^+$ ions were analysed with no energy filtering at a mass resolution $M/\Delta M$ of ≈1400. Because of the thinness of the deposit, a stable secondary signal was only obtained if the primary beam was rastered over a 100 × 100μm area. Each $^{11}B/^{10}B$ measurement was made of 10 blocks of 10 cycles with counting times of 8 s per cycle at mass 10 and 4 s at mass 11. Under these conditions, the precision obtained on the $^{11}B/^{10}B$ ratios ranges between ±0.2 and ±3.0‰ (1σ) for precipitation samples (Table 1). On the WHOI 1270 ion probe, a primary beam of O^- was delivered onto the sample with a nominal accelerating voltage of 12.5 kV. Secondary ions were extracted into the mass spectrometer through a nominal potential of 10 kV. Signals were collected cyclically, by magnetic switching, for the following analysed peaks: 9.33 (background, 1 s), $^{10}B^+$ (6 s) and $^{11}B^+$ (4 s). Waiting times of 0.5–1.0 s were allowed before counting each peak, to permit magnet settling. Measurements were made for about 80 cycles (25 min), depending on the concentration of B in the sample and the thickness of the deposit. B peak intensities and stability of measured $^{11}B/^{10}B$ were both monitored during each analysis for any indication of either hitting the silicon wafer or major drift of the signal. The instrument was operated with a mass resolving power in excess of 2000, to eliminate selectively isobaric interferences, in particular the interference of $^{10}BH^+$ on $^{11}B^+$. On both ion probes, the instrumental mass fractionation of

Table 1
Cl, Na, Ca, Mg, B concentrations and $\delta^{11}B$ and δD of atmospheric precipitations such as rains (†), snows (°), snow packs (°°) and freezing rains (††)

Sample	Sampling date	Altitude	km/sea	B (ppb)	$\delta^{11}B$ (‰)	±(1σ)	δD (‰)	Cl (ppb)	Na (ppb)	Ca (ppb)	Mg (ppb)	Na/Cl
Seawater				4500	39.6	1.0		2×10^7	1×10^7	4×10^5	1×10^6	0.56
Asia (Nepal)												
KTM 1†[d]	Monsoon 1997, nf[a]	1310	600	0.1	+3.6	2.5	−88	58.1	18	n.d.[b]	8.4	0.31
KTM 4†[d]	Monsoon 1997, nf[a]	1310	600	0.7	+11.2	1.3	−80	669.9	106	n.d.	25.4	0.16
LO225°	Jun. 5, 1993	4107	600	1.0	+18.5	1.7	−24	209.3	112	415.2	39.0	0.54
NAG 1†[d]	Nov. 10, 1995	1310	600	0.7	+6.0	0.6	−196	130.2	120	1257.5	100.0	0.92
NAG 2†	Nov.10, 1995	1310	600	0.2	+3.0	0.6	−158	180.3	130	339.3	15.0	0.72
NAG 53†[d]	Sept. 22, 1995	1310	600	3.0	+6.5	0.9	n.d.	330.5	140	7185.6	250.0	0.42
MO17bis†[d]	May 2, 1997	1000	700	1.2	+3.8	1.4	n.d.	64.1	83	858.3	145.0	1.29
MO 46°	May 6, 1997	3800	700	2.0	+23.0	1.6	n.d.	185.3	65	481.0	47.0	0.35
MO 62†[d]	May 7, 1997	3310	700	0.3	+6.5	0.4	n.d.	58.1	18	360.3	31.0	0.31
North America (Québec-California)												
Matagami°°	Mar., 1994	n.d.	410	1.0	+15.1	3.0	−102[c]	n.d.	38	n.d.	8.9	—
Lamothe°°	Mar., 1994	n.d.	500	2.2	−6.8	1.0	−62[c]	n.d.	388	n.d.	16.9	—
Opinaca°°	Mar., 1994	n.d.	220	1.6	+11.2	1.6	−110[c]	n.d.	579	n.d.	67.0	—
Chisasibi°°	Mar., 1994	n.d.	105	1.8	+6.8	1.3	−118[c]	n.d.	467	n.d.	138.0	—
L. Evans°°	Mar., 1994	n.d.	340	1.5	−10.2	0.5	−102[c]	n.d.	115	n.d.	18.3	—
Lac Koury°°	Mar., 1994	n.d.	45	2.0	+22.1	2.7	−80[c]	n.d.	662	n.d.	118.0	—
LAS 4°°	Dec. 25, 1997	40	800	0.2	+5.6	n.d.	−114[e]	165.4	42	n.d.	2.7	0.25
LAS 7††	Jan. 7, 1998	40	800	0.1	−0.1	n.d.	−121[e]	509.5	150	n.d.	8.2	0.29
LAS 8††	Jan. 8, 1998	40	800	0.1	+1.0	n.d.	−121[e]	168.7	93	n.d.	6.2	0.55
LAS 9††	Jan. 10, 1998	40	800	0.7	+3.9	0.5	−121[e]	379.8	183	n.d.	7.7	0.48
LAS 10°	Jan. 13, 1998	40	800	1.6	−0.3	0.2	−121[e]	434.9	179	n.d.	16.6	0.41
LAS 12°	Feb. 12,1998	40	800	0.3	+34.4	0.2	−121[e]	854.5	485	n.d.	18.7	0.57
LAS 13†	Jan. 16, 1998	40	800	1.0	+10.5	2.7	−121[e]	356.5	169	n.d.	16.3	0.47
LAS 14°	Feb. 20–25, 1998	40	800	0.4	−4.8	1.0	−121[e]	215.4	96	n.d.	9.5	0.45
LAS 16†	Mar. 9, 1998	40	800	0.3	−1.5	0.4	−98[e]	94.7	16	n.d.	5.0	0.17
97-CA-2†	Dec. 10, 1997	1	0	1.9	+26.0	0.5	−50[c]	2608.5	1490	n.d.	133.0	0.57
97-CA-3†	Dec. 10, 1997	1	0	1.5	+19.8	1.3	−50[c]	1815.1	962	n.d.	88.0	0.53

The $\delta^{11}B$ of the underlined samples were measured at CRPG-CNRS by ion probe Cameca 3f, all the others $\delta^{11}B$ were measured at WHOI by ion probe Cameca 1270. δD were measured at CRPG except for the Quebec samples.
[a] nf, non filtered.
[b] n.d., not determined.
[c] Values calculated using Rozanski et al. (1993).
[d] Rose et al. (2001).
[e] Based on data for Ottawa from the GNIP Database (GNIPmonthly), accessible at http://isohis.iaea.org.

$^{11}B/^{10}B$ was corrected for by comparison with intraday measurements of a synthetic glass standard GB4, for which the precision was better than ±1‰ (Chaussidon et al., 1997; Rose et al., 2001). B isotopic ratios are hereafter given in $\delta^{11}B$ notation, i.e., given in permil variations relative to the SRM951 boric acid standard whose $^{11}B/^{10}B$ ratio is accepted to be 4.04558 (Catanzaro et al., 1970).

Hydrogen isotopic composition of the condensate vapour was determined after water was converted to H_2 over uranium at 800 °C. H_2 gas was analysed on a VG 602D mass spectrometer at CRPG (France). The reproducibility for H on water samples was ±2‰.

4. Results

4.1. Boron concentrations of natural rains and snows

B concentrations in instantaneous rains range from 0.1 to 3.0 ppb (Table 1). They are not significantly different from those (0.2–2.2 ppb, Table 1) observed in instantaneous snows and snow packs, the latter representing an average atmospheric signal because they are cumulative deposits. The B concentration in rains ranges from 1500 to 4500 times less than in seawater (3000 times less on average). Table 1 also displays the analyses for Na, Ca, Mg and Cl of the precipitation samples, elements selected to help quantify the potential contributions of seawater or marine salts and non-marine particulate matter to these samples. Values for Cl range from 58 to 2609 ppb with the highest values coming from the shoreline rains near San Francisco. Na varies from 16 to 1490 ppb, with again the highest values being associated with the same shoreline rains. As classically observed in atmospheric precipitations (e.g. Rose et al., 2000a), Na and Cl in the rains are strongly positively correlated along a line with a slope close to the seawater Na/Cl ratio (Fig. 1a) indicating, at variance with other elements, the dominant marine control on atmospheric Na and Cl (e.g., Berner and Berner, 1996). The rains from near San Francisco have seawater type ratios of 0.56; however, only about half of the 20 rains and snows analysed

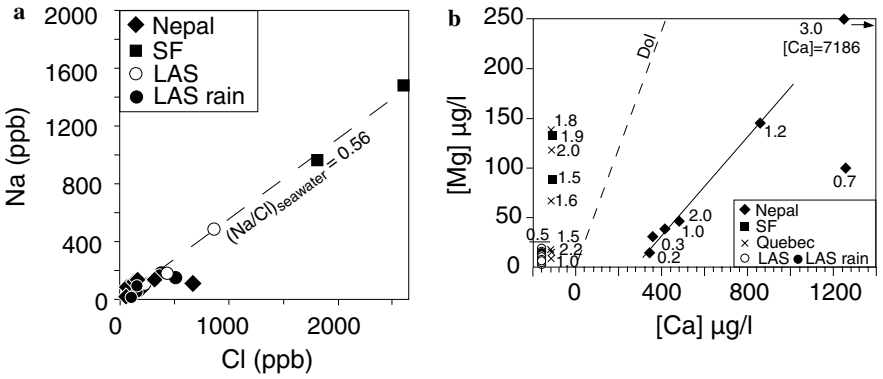

Fig. 1. (a) Cl concentration in precipitation as a function of Na concentration. Na and Cl in the precipitations are strongly positively correlated along a line (dashed line) with a slope corresponding to the seawater Na/Cl ratio (0.56). This indicates the dominant marine control on atmospheric Na and Cl in these samples. (b) Mg concentration in precipitations as a function of Ca concentration. Nepalese, San Francisco (SF) and LAS (Montreal) rains are represented by filled symbols whereas snow and freezing rains are represented by crosses for Quebec and open symbols for LAS. Samples for which Ca concentration data are not available, are plotted arbitrarily at [Ca] = −160 for LAS samples and [Ca] = −120 for San Francisco and Quebec precipitations. Although the data are limited to Nepal (black diamonds), Ca increases with increase in Mg with a good correlation for values of Mg between 8 and 150 ppb, suggesting that they are coupled. For the two high Ca (>900 ppb) rains, presumably independent sources for Ca and Mg are implied. The dashed line represents the dolomite line. Data points plotting on this line would have been associated with dissolution of dolomitic particles/aerosol in rain. Numbers aside the data points are the respective B concentration in ppb and the underlined value of 0.5 is the average B concentration for all the LAS precipitations. There is a tendency for the B concentration to increase with increase in Mg content, with the exception of Lamothe snow.

(Table 1) also have similar ratios. Both snows and rains have ratios that are significantly higher or lower than 0.56; certain of these samples are related to the monsoon precipitations of Nepal.

Ranges for Ca and Mg are 339–1258 ppb (an extreme value at 7186 ppb) and 3–100 ppb (extreme value at 250 ppb), respectively. The San Francisco shoreline rains have Mg/Cl weight ratios of about 0.05, which are smaller than the seawater ratio of 0.067, thus suggesting that even for shoreline rains the chemical composition of precipitations is not a simple dilution of seawater chemistry. This is of course more obvious for precipitations over the continents: Ca/Mg weight ratios for Nepalese rains range from 6 to 29, average of 10 excluding two values >20, i.e., in complete contrast with both the seawater ratio of 0.32 and the ratio of about 0.4 in oceanic rains (e.g., Berner and Berner, 1996). Although the data are limited to Nepal, Ca increases with increase in Mg (Fig. 1b), with a good correlation for values of Mg between 8 and 150 ppb, suggesting that they are coupled. This increase is followed by a moderate and a dramatic increase in Ca for two samples relative to no or moderate increase in Mg (NAG1 and NAG53, Table 1);for these two high Ca (>900 ppb) rains, presumably independent sources for Ca and Mg are implied.

The B/Cl molar ratio in precipitations, ranging from 6.4×10^{-4} to 6.1×10^{-2}, is highly variable relative to seawater (2.5×10^{-3}). The average B/Cl molar ratios of the precipitations from Nepal (0.021 ± 0.019) and Quebec (0.006 ± 0.004) are similar to those of lichens from Nepal and Quebec (0.028 ± 0.014 and 0.017 ± 0.011, respectively; Rose et al., 2000a).

The B concentrations of Table 1 are mostly similar to, but occasionally slightly lower than, previously reported rain data (0.8–9.4 ppb American Samoa; 0.5–15 ppb for Enewetak, Pacific; 0.3–12 ppb for Narragansett, Rhode Island; 3.2–8.6 ppb for Niwot Ridge, Colorado; Fogg and Duce, 1985). Rains from oceanic islands and coastal areas under direct marine influence, have B concentration on average higher than those from inland/continental areas (Fogg and Duce, 1985; Spivack, 1986; Miyata et al., 2000; Chetelat et al., 2005).

4.2. Hydrogen and boron isotopic compositions of rains and snows

The measured δD values of rains from Nepal range from −196 to −24‰. The wide range of δD values reflects in part the altitude variations from 1310 to 4107 m. A shoreline rain from California, 97-CA-2 has a δD of −50‰ and a snow pack from near Montréal, LAS 4, has a δD of −93‰ (Table 1).

The boron isotopic composition of instantaneous rain samples range from −1.5 to +26.0‰ (Table 1). The range for $\delta^{11}B$ of snow and snow pack samples is from −10.2 to +34.4‰ and is larger than that of rains. The two Californian shoreline (97-CA-2 and 97-CA-3) rains have very positive $\delta^{11}B$ values of +26.0 and +19.8‰, respectively (Table 1). The first Californian rain water was collected about 10 min after the rain started, and the second about 15 min later. Their $\delta^{11}B$ values are nonetheless significantly different with a 6‰ decrease between the first and second sample. The $\delta^{11}B$ values of the Nepalese instantaneous rains are tightly clustered between +3.0 and +6.5‰, despite the large range of Na/Cl from 0.16 to 1.30 (Table 1). Samples collected in Katmandu (NAG 2, 53 and the 2 KTM) are indistinguishable from the other

Nepalese samples in terms of both $\delta^{11}B$ and B concentrations, although anthropogenic B pollution cannot be ruled out because they were sampled downtown Katmandu. The instantaneous rains from Quebec have $\delta^{11}B$ values ranging from −1.5 to +10.5‰.

Fig. 2a compares the B concentrations of a total of 40 precipitations with their $\delta^{11}B$ values (Table 1), and includes previous data on equatorial and low latitude coastal rains of Spivack (1986) and Chetelat et al. (2005). Ninety percent of these samples (the shaded area on Fig. 2a, which excludes four outliers) show a general tendency of increasing $\delta^{11}B$ with increasing B concentration. For reference, a regression line is given. This global trend is also underlined by the concomitant increase in Cl concentration (Fig. 2b).

No well defined trends are observed between the $\delta^{11}B$ values of rains and/or snows and their Ca or Mg contents or, for example, their Na/Cl ratios. Nevertheless, the three rain samples with seawater like Na/Cl ratios of 0.56 ± 0.10 have relatively high $\delta^{11}B$ values with $+10 < \delta^{11}B < +26$‰. Adding the freezing rain and snow data with Na/Cl ratios of ~0.56 extends the range of rains with marine like Na/Cl to $0 < \delta^{11}B < +34$‰. All precipitations with Cl > 700 ppb have seawater type Na/Cl ratios and $\delta^{11}B$ values >+19‰, including the two shoreline samples from near San Francisco.

Fig. 3 examines relationships between $\delta^{11}B$ and the molar ratio Mg/B and includes data for seawater (Mg/B = 126 and $\delta^{11}B = +39.5$‰). The two marine samples from California and the instantaneous snow samples (2 from Nepal and 3 from Quebec) plot on a trend with a steep slope (Fig. 3). Other rain samples with a clear marine affinity, i.e., samples from the wet season from Guiana (Chetelat et al., 2005), also plot on this trend. A regression line (trend I) was drawn on Fig. 3 for all these samples showing a strong co-variation between $\delta^{11}B$ values and Mg/B ratios. A trend with a much smaller slope (trend II, Fig. 3) can be defined for the Nepalese instantaneous rains and the three freezing rains from Quebec. Note that the rains on each trend have distinctive Cl concentrations. In general, along trend I lie the rains with [Cl] > 300 ppb whereas along trend II lie the rains with [Cl] < 300 ppb. Seawater does not plot near either of the two extrapolated trends but in between.

The range of $\delta^{11}B$ values derived from the data of Table 1 covers most of that previously available: +0.8 to +35‰ for rains from the Pacific islands of Guam, Enewetak and

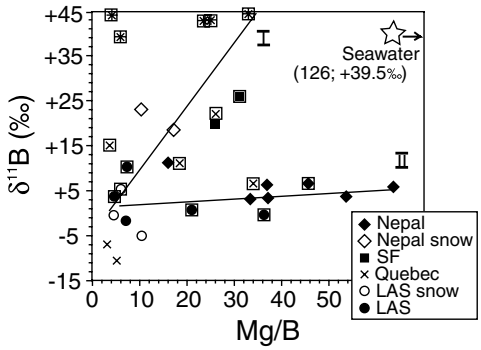

Fig. 3. Variation of boron isotopic composition in natural precipitations as a function of Mg/B molar ratio. Seawater, represented by a star, plots way to the right of the upper right hand corner of the figure. Other symbols are the same as in Fig. 2a. The two shoreline rains from San Francisco and Nepalese snows and half of the snow packs plot along regression line I with $\delta^{11}B$ values from +5‰ to +45‰. The $\delta^{11}B$ values of Nepalese rains, with the exception of KTM4, plot along regression line II, going from low $\delta^{11}B = 0 \pm 5$‰ and low Mg/B < 10 to $\delta^{11}B < +10$‰ and high Mg/B > 60. This trend starts in the same low $\delta^{11}B$-low Mg/B left hand corner as line I. If the Mg/B ratio of trend II is largely controlled by particulate aerosols, then the range of $\delta^{11}B$ values of inland aerosols is quite restricted at +7 ± 4‰ whether from Nepal or Quebec (see Section 5 for details). Along line II all precipitations have [Cl] < 300 ppb and along line I precipitations have [Cl] > 300 ppb. Samples boxed in open squares are taken from Fig. 4.

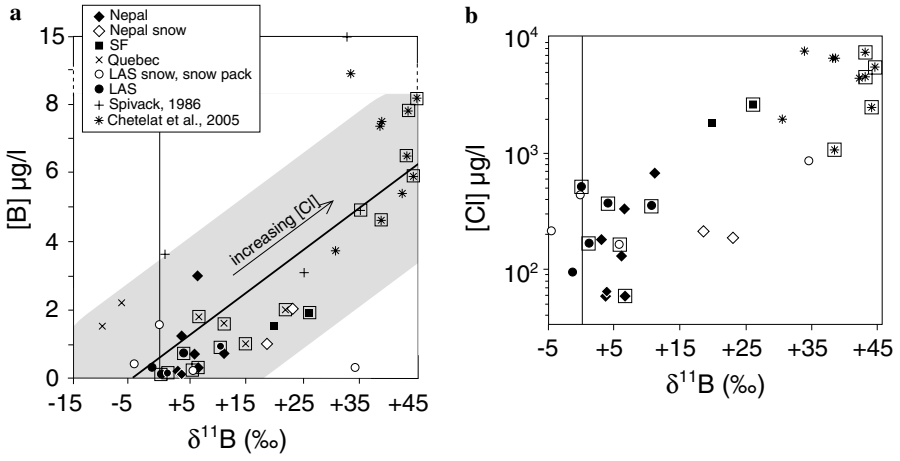

Fig. 2. (a) B concentrations of precipitations as a function of their $\delta^{11}B$. Previous data on equatorial and low latitude coastal rains of Spivack (1986) and Guiana rains of Chetelat et al. (2005) are also reported (as plus signs and star symbols, respectively). All other solid symbols are rains. A regression line is given for reference that is based on the 36 samples in the grey area among the 40 represented. Samples boxed in open squares are taken from Fig. 4. (b) Cl concentration (µg/l) as a function of their $\delta^{11}B$. Thirty samples from (a) for which data exist, are represented on this figure with the same symbols as in (a). Cl concentration in precipitation increases with the $\delta^{11}B$. The variations of Cl concentration span over two orders of magnitude while $\delta^{11}B$ varies from −5 to +45‰. Samples boxed in open squares are taken from Fig. 4.

Fanning, and +2.3‰ for the Orinoco basin (5 samples; Spivack, 1986); a rain at +16.7‰ for Da Qaidam in China (Xiao et al., 1992); +18.9 to +34.7‰ for N.W. Pacific oceanic rains (Miyata et al., 2000). Recently, Chetelat et al. (2005) reported values for coastal rains during the wet and dry seasons near Cayenne in French Guiana with high $\delta^{11}B$ ranging from +30.6 to +44.8‰ and B concentrations from 3.7 to 13.9 ppb. The average $\delta^{11}B$ of the Guiana rains during the wet season is higher than that during the dry season ($+42.7 \pm 2.2$‰ and $+35.4 \pm 3.9$‰, respectively; Chetelat et al., 2005).

Only the study by Miyata et al. (2000) reports $\delta^{11}B$ values of both oceanic rains and marine air (NW Pacific Ocean and coastal locations in Japan). Average $\delta^{11}B$ of four open ocean rains ($+26 \pm 6$‰) are on the order of 31‰ heavier than the average $\delta^{11}B$ of four open ocean atmospheric vapours (-5.4 ± 1‰).

All the $\delta^{11}B$ data of Table 1 and the above published data that can be assigned with δD values, measured or calculated from the $\delta^{18}O$ data, and in large part from the literature (Dansgaard, 1964; Rozanski et al., 1993; IAEA/WMO, 2004) are presented on a $\delta^{11}B$ versus δD plot in Fig. 4. Guiana rains have an average δD of -14 ± 12‰ during the dry season and -21 ± 15‰ during the wet season (Négrel et al., 1997). No simple relationship is observed between $\delta^{11}B$ and δD. However, considering only the rain data, the highest $\delta^{11}B$ value for a given value of δD does decrease systematically with decreasing δD value. The only conspicuous exceptions are two Nepalese rains which both have ≪1ppb of B and low $\delta^{11}B$ values (Table 1). The highest $\delta^{11}B$—highest δD values of rains are similar to those of seawater and restricted to low latitudes, and lower $\delta^{11}B$—lower δD values of rains correspond to higher latitudes, altitudes and/or distances from the ocean. As in Figs. 2a and b, for precipitations with $\delta^{11}B < +10$‰, the data become more dispersed.

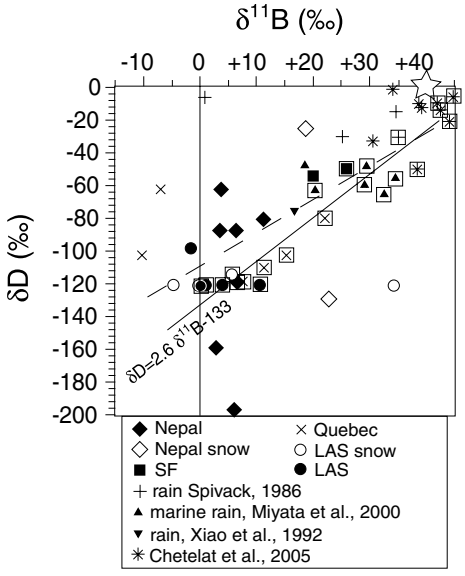

Fig. 4. Plot of δD as a function of $\delta^{11}B$ for precipitations from Table 1 and the literature. δD values are measured or calculated from the $\delta^{18}O$ data, and are in large part from the literature (Dansgaard, 1964; Rozanski et al., 1993; Négrel et al., 1997; IAEA/WMO, 2004). No simple relationship is observed between $\delta^{11}B$ and δD. However, considering only the rain data, the highest $\delta^{11}B$ value for a given value of δD does decrease systematically with decreasing δD value. Rains with the highest $\delta^{11}B$—highest δD values are marine precipitations (and seawater) at low latitudes, and rains with lower $\delta^{11}B$—lower δD values correspond to precipitations at higher latitudes, altitudes and/or distances from the ocean. A linear relationship between δD and $\delta^{11}B$ ($\delta D = 2.6\delta^{11}B - 133$; the boron meteoric water line) has been added to the figure (see Section 5.1 for details). A regression line through all the samples that formed the correlation of Fig. 2a (grey area), gives a relationship ($\delta D = 2.0\delta^{11}B - 109$; dashed line) that is close to $\delta D = 2.6\delta^{11}B - 133$ (solid line) and particularly for $\delta^{11}B > +5$‰. Samples boxed in open squares have the most negative δD value for any given $\delta^{11}B$ value, excluding just four outliers. A regression line through them gives a relationship that is indistinguishable from $\delta D = 2.6\delta^{11}B - 133$, to within the analytical uncertainties. Symbols are the same as in previous figures with a star for seawater.

5. Discussion

5.1. Boron meteoric water line

The trend on Fig. 4 which is more clearly defined for high δD—high $\delta^{11}B$ values, is considered to be of note because of possible analogies with the global meteoric water line for δD and $\delta^{18}O$; the relationships between δD and/or $\delta^{18}O$ and latitude and/or altitude, or mean annual air temperature, is reproduced by Rayleigh condensation models, or extensions to them, and the currently available global atmospheric circulation models (e.g., Dansgaard, 1964; Rozanski et al., 1993). For the global meteoric water line ($\delta D = 8\delta^{18}O + 10$; Craig, 1961) the slope of 8 is related to the ratio of the hydrogen and oxygen isotope fractionation factors between vapour and liquid. By analogy with the meteoric water line, the relationship $\delta D = 2.6\delta^{11}B - 133$ can be derived between δD and $\delta^{11}B$ (Fig. 4). As a first approximation, the slope of 2.6 has been derived from the ratio of the vapour–liquid fractionation of −80‰ for hydrogen (Craig and Gordon, 1965) to −31‰ for boron, the latter being derived from the open ocean gas-rain data of Miyata et al. (2000). Note that in this model, the rain is enriched in D and ^{11}B relative to the atmospheric vapour reservoir. Contrary to the slope of 2.6, the intercept of the line in δD–$\delta^{11}B$ space has a priori no simple physical meaning. It was determined at $\delta D = -133$‰ for $\delta^{11}B = 0$‰, taking as a fixed point on the line the average values of Guiana wet season rains ($\delta D = -21 \pm 15$‰ and $\delta^{11}B = +42.7 \pm 2.2$‰; Négrel et al., 1997; Chetelat et al., 2005). These rains come directly from the Atlantic Ocean that is 400 m from the sampling station. At present, they represent the best available samples of equatorial rains which have escaped a protracted evolution in the atmospheric reservoir.

As shown in the following, such a "boron meteoric water line" is in good agreement with most of the available worldwide δD–$\delta^{11}B$ rain data. A regression line through all the samples that form the correlation of Fig. 2a (grey area), gives a relationship ($\delta D = 2.0\delta^{11}B - 109$; dashed line on

Fig. 4) that is close to $\delta D = 2.6\delta^{11}B - 133$ (solid line on Fig. 4) and particularly for $\delta^{11}B > +5‰$. Alternatively, samples can be selected that have the most negative δD value for any given $\delta^{11}B$ value, excluding just four outliers. These samples are boxed in open squares on Fig. 4. A regression line through them gives a relationship that is indistinguishable from $\delta D = 2.6\delta^{11}B - 133$, to within the analytical uncertainties, and is thus not shown on Fig. 4. These same samples are marked on Figs. 2a and b where they are seen to follow the trend of increasing boron or chlorine concentration with increase in $\delta^{11}B$ values. On Fig. 3, the majority of these samples plot around trend I (symbols are also boxed in open squares). The combination of the trends for these samples suggests that all these parameters are related by common processes. These three derivations only share the Guiana data. The derivations of the slopes of 2.6 are completely independent of each other. Such a coincidence is considered improbable unless all derivations share common boron and hydrogen isotope vapour–liquid isotope fractionations. For these reasons, additional confidence is given to the value of about −31‰ for the vapour–liquid boron isotope fractionation during precipitation processes. The relationship $\delta D = 2.6\delta^{11}B - 133$, that will subsequently be referred to as the boron meteoric water line, also implies that at least part of the $\delta^{11}B$ values of precipitations can be satisfactorily modelled by a Rayleigh process.

The third method given above for deriving a slope of 2.6 in δD–$\delta^{11}B$ space is essentially identical to that used by Craig (1961) to determine the numerical coefficient of 8 for the slope in δD–$\delta^{18}O$ space. It was based on the measurements on global meteoric waters, and then loosely related to the ratio of the vapour–liquid hydrogen and oxygen isotope fractionation factors. Because both the δD and $\delta^{18}O$ values of precipitations give excellent linear correlations with annual mean air temperature at the surface for temperatures between +25° and −50 °C (Dansgaard, 1964), the slope of 8 is insensitive to surface temperature variations. However, even over the limited temperature range of +25° to −6 °C, which is roughly equivalent to δD of precipitation changing from 0 to −133‰, the ratio of the hydrogen and oxygen isotope liquid–vapour fractionations changes from about 8 to 9.6 (Friedman and O'Neil, 1977). Thus the slope of 8 is not simply related to the ratio of the fractionations and their variations with temperature. In detail, the liquid–vapour fractionations for hydrogen and oxygen isotopes during evaporation of seawater are similar to but not identical to the equilibrium values (Craig and Gordon, 1965), but this difference is probably of secondary importance here. By analogy with the slope of 8, the satisfactory quality of the boron meteoric water line and the present state of understanding, the slope of 2.6 is also considered to be insensitive to variations in the annual mean air temperature of the surface.

Compared with the high quality of the relationship between δD and $\delta^{18}O$ for precipitations, the lower quality of the systematic relationship between $\delta^{11}B$ and δD in general (Fig. 4) implies that only part of the $\delta^{11}B$ signal can be related to the isotopic evolution of the cloud system by a Rayleigh model. In particular, many precipitations with $\delta^{11}B < +10‰$ and low B concentrations of <2 ppb (Fig. 2a) cannot be just described by such a model. This is not surprising noting that (1) hydrogen is a major element with no change of concentration during a Rayleigh process in contrast to boron, a trace element, and (2) it is known that up to about 10% of atmospheric boron can come from oceanic and/or continental aerosols, and volcanic, biogenic and anthropogenic sources (Fogg and Duce, 1985).

5.2. Speciation effects and liquid–vapour B isotope fractionations

The speciation of dissolved boron in normal seawater is well studied (e.g., Spivack and Edmond, 1987; Hemming and Hanson, 1992), with only two dominant species (~59% $B(OH)_3$ and ~41% $B(OH)_4^-$) that are interrelated by:

$$B(OH)_3 + H_2O = B(OH)_4^- + H^+ \quad (1)$$

There is an isotopic fractionation of about 20‰ between these two B species, with $B(OH)_3$ concentrating ^{11}B. Small changes of a few tenths of a pH unit around the normal seawater value of 8.3 markedly change the distribution of $B(OH)_3$ and $B(OH)_4^-$ in solution and hence their individual isotopic compositions. Because both rains and sea salt particles have relatively low pHs, ranging from 4 to 6 (e.g., Fogg and Duce, 1985) and 5 to 6 (Eriksson, 1957), respectively, $B(OH)_3$ is by far the dominant species in them. The speciation of B in atmospheric vapour is not well documented but is widely considered to be $B(OH)_3$ because this species in seawater is neutral and therefore taken to be by far more volatile than $B(OH)_4^-$ (Fogg and Duce, 1985). We can thus consider in the following that the B isotopic fractionation taking place in the atmosphere between rain and vapour is mostly that between $B(OH)_3$ dissolved in liquid water and gaseous $B(OH)_3$, i.e., $\Delta_{\text{vapour–rain}} = \Delta_{\text{gaseous B(OH)}_3\text{–dissolved B(OH)}_3} = -31‰$.

The most ^{11}B enriched rains known ($\delta^{11}B = +45‰$), come from the equatorial coastal station at Cayenne, Guiana (Chetelat et al., 2005). They are also among the most enriched rains in D, at −5‰ (Négrel et al., 1997). Taking +45‰ as a good estimate of the upper limit for $\delta^{11}B$ of the first rains gives, for a $\Delta_{\text{vapour–rain}} = -31‰$, a $\delta^{11}B$ value of +14‰ for the initial isotopic composition of atmospheric vapour derived from the ocean before the initiation of significant condensation–precipitation processes. Comparing this $\delta^{11}B$ value of +14‰ with that of seawater ($\delta^{11}B = +39.5‰$) gives about −25.5‰ for the vapour–seawater fractionation. The difference between the two liquid–vapour fractionations of −31 and −25.5‰ can be related to speciation effects. Under the normal pH conditions of seawater, $B(OH)_3$ is about 5.5‰ enriched in $\delta^{11}B$ compared with the total boron ($\Sigma[B(OH)_3 + B(OH)_4^-]$) in seawater

(Hemming and Hanson, 1992) so that $\Delta_{\text{vapour–seawater}} = \Delta_{\text{gaseous B(OH)}_3\text{–dissolved B(OH)}_3} + \Delta_{\text{dissolved B(OH)}_3\text{–seawater}} = -31‰ + 5.5‰ = -25.5‰$. This difference supports the dominance of $B(OH)_3$ in the vapour and can explain why the first Guiana rains can have $\delta^{11}B$ values around +45‰. This also implies that there is no significant apparent fractionation between dissolved $B(OH)_3$ in seawater and boron in the first rains. The above fractionations combined with the processes described by the boron meteoric water line can explain the fact that rain waters can have $\delta^{11}B$ values both enriched and depleted in ^{11}B relative to the seawater source.

5.3. Temperature effects and liquid–vapour B isotopic fractionations

As shown previously, B isotopic compositions of atmospheric precipitation imply that the vapour is depleted in ^{11}B relative to the liquid, whether seawater or rain. Except for the preliminary experimental data of Xiao et al. (1992), where seawater was evaporated at 25 and 35 °C, using an air-flow system, all previously derived liquid or brine-vapour B isotope fractionations are in the opposite sense, with the vapour enriched in ^{11}B relative to the aqueous solution (Fig. 5). The experimental data are, however, only relevant for temperatures higher than about 125 °C. They were derived from laboratory experiments between brine and its vapour at 425–450 °C by Spivack et al. (1990), and from empirical experiments between saline or hypersaline brines and their associated vapours from several geothermal systems by Leeman et al. (1992). Combining our data with these data as a whole therefore imply that there is a crossover in the B isotope saline liquid–vapour fractionation between surface temperatures and 125 °C. Xiao et al.'s (1992) preliminary fractionation data (≈13‰; inverse open triangle on Fig. 5) support our data (25 and 31‰; filled circles on Fig. 5) that the vapour is depleted in ^{11}B relative to seawater at surface temperatures but their values are smaller. The differences among these values are difficult to interpret in the absence of more detailed information on their experimental set up. It is noted that Xiao et al. report that their fractionation decreases with decrease in temperature, which is rather unusual.

Most of the B isotopic variability of rains, with a range of $\delta^{11}B$ values from +45‰ to −13‰ that is observed for worldwide precipitations, can be readily accounted for by vapour–liquid fractionation factors (α) of about 0.9754 for seawater and about 0.9703 for precipitations, and the dominance of a Rayleigh distillation process which result in the observed boron meteoric water line.

5.4. Implications on atmospheric boron concentrations and sources

The present B isotopic fractionations, $\Delta_{\text{vapour–seawater}} = -25.5‰$ and $\Delta_{\text{vapour–rain}} = -31‰$, have strong implications regarding the origin and evolution of atmospheric B that can be inferred from existing rain B isotopic data. Fig. 6 presents the measured values of gaseous B in the marine atmosphere from the data of Miyata et al. (2000). These results were interpreted in terms of a two, or possibly more, end members mixing model between (1) a low B concentration and high $\delta^{11}B$ component that could only be proposed to have a $\delta^{11}B$ value > 0‰, and (2) a high B

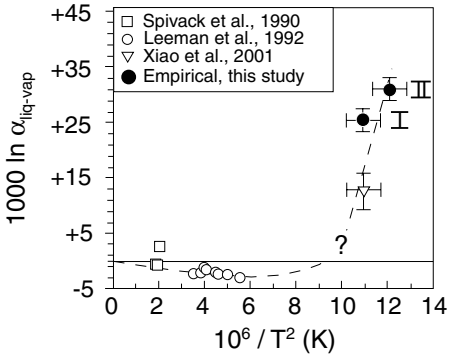

Fig. 5. Experimentally and empirically determined boron isotope fractionation factors between aqueous liquids and vapour ($\alpha_{\text{liq–vap}}$) in the temperature range of 450 °C to ≈20 °C. The empirical fractionation data (from Section 5.1 and Fig. 4; see Section 5) are solid circle I, representing the seawater–vapour fractionation ($1000\ln\alpha_{\text{sw–v}} = +25.5$) shown for 30 °C ($10^6/T^2 = 10.89$), and solid circle II, the rain water–vapour fractionation ($1000\ln\alpha_{\text{r–v}} = +31$) shown for 15 °C ($10^6/T^2 = 12.06$). The high temperature data are from the experimental measurements between co-existing brine and its vapour of Spivack et al. (1990; open squares), and empirical measurements on brine and its vapour from various geothermal springs of Leeman et al. (1992; open circles). Laboratory experiments at 25 and 35 °C, averaged at 30 °C for clarity, are from Xiao et al. (2001). A crossover in the aqueous liquid or brine–vapour fractionation is implied at temperature between 40 and 125 °C, although it is noted that the chemistry of the liquid at the different temperatures is not strictly comparable.

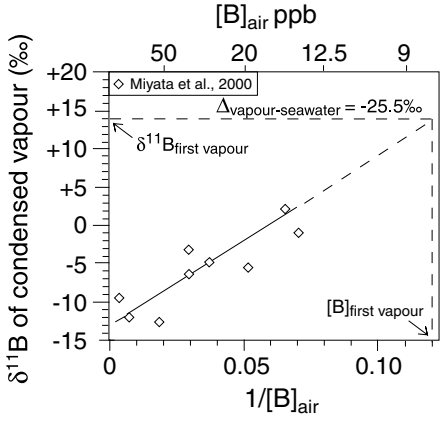

Fig. 6. The $\delta^{11}B$ value of marine air as a function of 1/[B] from Miyata et al. (2000) with their correlation line. It is here interpreted in terms of the dominance of a Rayleigh process with a −31‰ fractionation between vapour and precipitation. Not only does $\delta^{11}B$ decrease with increase in evolution of the atmospheric reservoir but also, as observed, the boron concentration in the vapour increases concomitantly because measured boron concentrations in the atmosphere are from 20 to 2 times higher than their rains. Applying the proposed $\delta^{11}B$ value of +14‰ for the initial vapour derived from seawater to the extrapolated regression line indicates that the initial vapour had a boron concentration of about 8 ppb.

concentration component having a low $\delta^{11}B$ value of about $-12‰$. However, Miyata et al. (2000) did not attempt to identify the nature of either end member. As an alternative explanation they suggested that a Rayleigh model could explain the $\delta^{11}B$ results so long as the vapour–liquid fractionation was more negative than $\sim -10‰$ as observed by Xiao et al. (2001). A negative $\Delta_{vapour-rain}$ implies that atmospheric $\delta^{11}B$ decreases with increase in evolution of the atmospheric reservoir. Concomitantly, and as observed in Miyata's data (see Fig. 6), the boron concentration in the vapour must increase because measured boron concentrations in the atmosphere are from 20 to 2 times higher than their rains. Applying the proposed $\delta^{11}B$ value of $+14‰$ for the initial vapour derived from seawater to Fig. 6 indicates that the initial vapour had a boron concentration of about 8 ppb. This interpretation of Miyata et al.'s (2000) marine data implies that these samples represent atmospheric vapours that have already undergone significant evolution or distillation from the initial vapour reservoir. This is coherent with their latitudes of 38° to 47 °N that are substantially removed from their equatorial source region.

It is possible to calculate the boron concentration in the atmosphere (gas) assuming (1) the boron concentration in sea-salts, and (2) boron evaporates from sea-salts as gaseous $B(OH)_3$. Henry's law constant H_c in the equation

$$[B(OH)_3]_{gas} = H_c \times [B(OH)_3]_{sea-salt} \quad (2)$$

is 4.7×10^{-9} for $B(OH)_3$ at 25 °C in seawater (assuming the activity coefficient of boric acid is 1, and $[B]_{seawater} = 4.5$ g/m^3). Using the Van't Hoff equation of the enthalpy of reaction, one can calculate that H_c varies from 2.8×10^{-9} to 6.2×10^{-9} for temperatures of 10 and 30 °C, respectively. If the salinity of the sea-salt is that of seawater (i.e., $[B] = 4.5$ ppm; therefore at sea-salt pH of 5, $[B(OH)_3]_{sea-salt} \approx 4.5$ ppm $= 4.5$g/m^3) then the variation in temperature from 10 to 30 °C corresponds to an increase in gaseous $B(OH)_3$ concentration of 12.6 ng/m^3 of air (i.e., 9.7 ppb because 1m^3 of air weights 1.3kg) to 27.9 ng/m^3 of air (i.e., 21.5 ppb; using Eq. (2)). These values are very similar to or higher than the 8 ppb B concentration derived from Fig. 6. Values higher than 8 ppb B could be due to the addition of sea/salt droplets to the atmosphere. Because the sea-salts/droplets are drying in air, their water evaporates, and some authors propose that up to seven eighths of their water evaporates (i.e., $[B]_{sea-salt}$ up to 36 ppm; Junge, 1963). In this case, for the same temperature range, the gaseous $B(OH)_3$ concentration varies between 78 and 172 ppb, values similar to or higher than the average 77 ppb gaseous boron concentration from coastal areas proposed by Fogg and Duce (1985). In both cases, it appears that sea-salts could always act as a source of boron to the atmosphere in the temperature range from 10 to 30 °C.

Finally, it is worth noting that the presently proposed concentration of boron in the initial vapour derived from the seawater reservoir (about 8 ppb) is lower than many measured coastal values which average 77 ppb (e.g. Fogg and Duce, 1985). Unfortunately, data on boron concentrations and $\delta^{11}B$ values of atmospheric gases above open ocean water at equatorial latitudes, where the major evaporation processes occur, are lacking. In the absence of these critical data, this difference in concentration can possibly be explained in terms of either a seawater aerosol contribution to the atmosphere or a Rayleigh process (Fig. 6). For example, the difference of 69 ppb (between the 77 ppb boron in the air from coastal region and 8 ppb of the initial open ocean vapour derived from seawater) could be supplied by a contribution of about 1.5% of aerosol to the atmosphere. The addition of this small percentage dominates the boron concentration and its $\delta^{11}B$ value in the atmosphere. In reality, the amount of aerosol added to the atmosphere is likely to be quite variable. This could account, in part, for the very large range of reported boron concentrations in the coastal and near coastal (e.g. Japan Sea) marine atmosphere.

5.5. Aerosols contribution to atmospheric boron

Rain is a complex mixture of liquid, gas and aerosols. For the boron system it is convenient to divide the aerosol contribution into two types: (1) aerosol droplets principally coming from seawater, and (2) particulate aerosols which are usually considered to be derived from sea salts, soil and volcanic dust, with the latter being principally an episodic contribution, and anthropogenic sources such as from burning of coal and forests. Seawater aerosols, before significant evaporation, contribute $\delta^{11}B$ values of $\sim +39.5‰$ with high concentrations of boron ($\sim$4500 ppb). Even from the existing limited data base for both $\delta^{11}B$ and [B] on worldwide precipitations, the direct seawater aerosol and/or sea salt particulate aerosol contributions can only be an extremely minor one except possibly in some coastal environments. For example, assuming that all the boron in Guiana rains ($\sim +43‰$, Fig. 2a) comes from aerosols gives a maximum contribution of 0.2%. Coastal rains in Florida with 75 ppb B could contain a maximum contribution of 1.7% seawater aerosol (Carriker and Brezonik, 1978). Partial water evaporation of seawater droplets before incorporation in rains adds a very small quantity of ^{11}B depleted vapour (initially $\sim +14‰$) relative to seawater plus liquid or solid aerosols with $\delta^{11}B$ like that of seawater. After a complete evaporation of droplets, the change in $\delta^{11}B$ is insignificant (see Section 3.2: preparation of samples by evaporation). Although Fogg and Duce (1985) estimated that 5 to 10% of the boron in the atmosphere is present in particulate form, liquid or particulate seawater aerosol can be no more than a trace to minor constituent of the total particulate material, except possibly in some coastal and oceanic settings. Unfortunately the data base here is either missing or too limited to explore this possibility.

The contribution of particles is examined here using the elements Mg and Ca that are influenced by both marine and continental sources in precipitations (e.g., Berner and

Berner, 1996). The dominance of a continental contribution to Ca and/or Mg to inland precipitation is illustrated in Fig. 1. Oceanic rains have a Ca/Mg weight ratio of about 0.45 (e.g., Berner and Berner, 1996) that is quite different from the average value of 12 for all the Nepalese rains and snows (Fig. 1). Although the Mg and Ca contents of many of the Nepalese rains and the two snows are related, they are not controlled by dolomitic particles (Fig. 1). Adsorption of B onto small clay particles may be important for controlling the $\delta^{11}B$ of rain and snow because it would result in significant increase of the precipitation's $\delta^{11}B$ value. However, their continental sources have not yet been identified, but if they are in part carbonate sediments then they are limestones. Because the B content tends to increase with increase in Mg and Ca, perhaps their $\delta^{11}B$ values can shed light here.

From their $\delta^{11}B$ and Mg/B values, Fig. 3 shows that the precipitations can be divided into two groups, giving trends I and II. All the precipitations with $\delta^{11}B > +10‰$ define trend I. Trend II includes many of the other precipitations with $\delta^{11}B < +10‰$. If the Mg/B ratio of trend II is largely controlled by particulate aerosols, then the range of $\delta^{11}B$ values of inland aerosols is quite restricted at $+7 \pm 4‰$ whether from Nepal or Quebec. Although such values are enriched in ^{11}B relative to average continental crust, some igneous and many sedimentary rocks (e.g., Palmer and Swihart, 1996) including loess (mostly within the range 0 to +10‰; Zhao et al., 2003) have similar values. The above range also overlaps that of fly ash leachates, derived from burning of coal and oil, with values from −19.2 to +15.8‰ (Davidson and Bassett, 1993). However, in the absence of additional data the contribution from this source cannot be assessed here. A minor contribution from sea salt aerosols cannot be totally excluded from some of the higher $\delta^{11}B$ samples, for example as seeds to snow samples, of trend I. Because the B contents of the precipitations are so low (<2–3 ppb) and the B contents of sea salt aerosols so high (>4500 ppb), the B sea salt aerosol contribution cannot be more than a percent or so of the total B in precipitations.

In Guiana, Chetelat et al. (2005) have shown that the dry season rains, which come from the southeast after crossing Brazil and central Guiana, have an average $\delta^{11}B$ value of $+35.4 \pm 3.4‰$, and are thus depleted in ^{11}B relative to both seawater and wet season rains. They invoked contamination of the rains by forest fires and/or anthropogenic B emissions. This interpretation is supported here because the decrease in $\delta^{11}B$ is probably not associated with a Rayleigh process as δD does not decrease too (Fig. 4). Part of the scatter observed for some other rains around the boron meteoric water line might also have this biogenic and/or anthropogenic origin (Fig. 7).

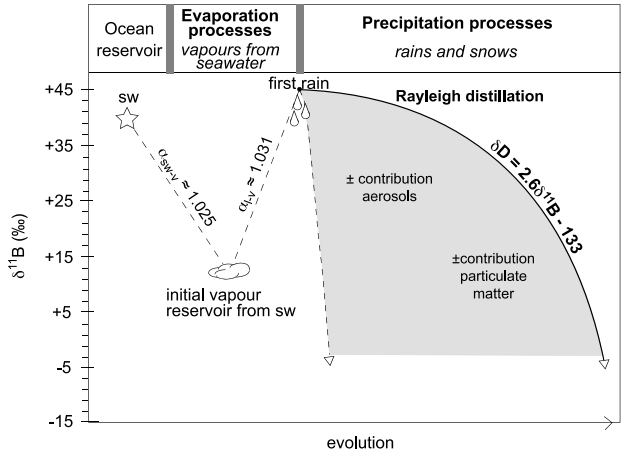

Fig. 7. Schematic model of ocean–atmosphere system for boron. The fractionation factors (α_{l-v}) associated with the evaporation of seawater ($\alpha_{sw-v} \approx 1.025$) and vapour–condensation processes ($\alpha_{l-v} \approx 1.031$) are shown giving the first rains at +45‰. The shaded area displays the evolution of $\delta^{11}B$ of precipitations as the $^{11}B/^{10}B$ ratio of the atmosphere evolves. The tendency of the curves is described by a Rayleigh process (the solid line of the shaded area related to $\delta D = 2.6\ \delta^{11}B - 133$), with more or less minor perturbing contributions from aerosols (natural and anthropogenic) and particulate matter (shaded area).

6. Conclusion

The large variations in the $^{11}B/^{10}B$ ratio of atmospheric boron, either as vapour or as precipitation, are related to the seawater boron reservoir via a combination of processes (Fig. 7): (1) the seawater–vapour fractionation ($\Delta_{vapour-seawater} \approx -25.5‰$), (2) the rain–vapour fractionation ($\Delta_{vapour-rain} \approx -31‰$), (3) evolution of the $\delta^{11}B$ value of the atmospheric vapour reservoir via evaporation–condensation-precipitation processes, which can be modelled as a Rayleigh distillation process, and that leads to the boron meteoric water line: $\delta D = 2.6\delta^{11}B - 133$, (4) any contribution of vapour from the evaporation of seawater aerosols, typically with $\delta^{11}B$ values around +14‰, and (5) any contribution from particulate matter, principally sea-salt and/or continental dust but, and probably more local or regional, anthropogenic and biogenic. Processes (1) and (2) are basic to all precipitations, and processes (3) to (5) either singly or in combination may be significant, both in marine and coastal, and continental precipitations. The seawater–vapour and precipitation–vapour fractionations are in general different because of changes in the speciation of boron between seawater (~59% $B(OH)_3$ and ~41% $B(OH)_4^-$), and precipitation and vapour, where boron is principally or wholly as $B(OH)_3$. The vapour concentrates ^{10}B relative to the liquid (seawater or rain) under atmospheric evaporation and condensation conditions, just like hydrogen and oxygen isotopes in comparable systems.

A sea-salt aerosol contribution, with assumed $\delta^{11}B$ value near +40‰, is possibly a major source of boron in the atmosphere above equatorial open oceans and along coastlines but, in the absence of basic data, the importance of this aerosol cannot be even semi-quantified. It has not been clearly identified in continental precipitations. If present, it must be less than a percent or so of the total boron. Dusts, anthropogenic, and volcanic contributions are possible

other sources of boron to the atmosphere. They can be locally or regionally important. Isotopically they are difficult to detect unless they do not plot along the boron meteoric water line.

In terms of mass balance for boron, the main terrestrial reservoirs are the continental crust (≈70% of the total B), oceanic crust (≈15%), upper mantle (≈12%), and the oceans (≈2%). Although the atmosphere and its precipitations are not a major B reservoir, they are important local sources of B to rivers and represent a relative B reservoir at least 3 orders of magnitude larger than that of rivers (Rose, 1999). For local B studies, atmospheric inputs to rivers could therefore have a noticeable impact on the B budget.

Acknowledgments

We thank in Nancy, Christian France-Lanord for the use of his hydrogen measurement facility and Pierre Coget for his help in performing hydrogen isotopic measurements, at WHOI, Nobumichi Shimizu for access to the 1270 ion probe, Graham Layne for technical advices, and Kenneth T. Koga for his useful comments. Support for EFR-K was provided by the French ''Programme Lavoisier'' post-doctoral scholarship and by a J. Steward Johnson scholarship from W.H.O.I., USA. Constructive reviews of an earlier version of this manuscript by J. Gaillardet has been very helpful. We thank four anonymous reviewers, Steve Galer and Rick Hervig for their constructive comments on the manuscript.

Associate editor: Richard L. Hervig

References

Berner, E.K., Berner, R.A., 1996. *Global Environment: Water, Air, and Geochemical Cycles*. Prentice-Hall, Englewood Cliffs, NJ.

Carriker, N.E., Brezonik, P.L., 1978. Sources, levels, and reactions of boron in Florida waters. *J. Environ. Qual.* **7** (4), 516–522.

Catanzaro, E.J., Champion, C.E., Garner, E.L., Malinenko, G., Sappenfield, K.M., Shields, W.R., 1970. Boric acid: isotopic, and assay standard reference materials. *Nat. Bur. Stand. Spec. Publ.* **260**, 17–70.

Chaussidon, M., Albarède, F., 1992. Secular boron isotope variations in the continental crust: an ion microprobe study. *Earth Planet. Sci. Lett.* **108**, 229–241.

Chaussidon, M., Robert, F., Mangin, D., Hanon, P., Rose, E.F., 1997. Analytical procedures for the measurement of boron isotope compositions by ion microprobe in meteorites and mantle rocks. *Geostand. Newslett.* **21** (1), 7–17.

Chetelat, B., Gaillardet, J., Freydier, R., Negrel, Ph, 2005. Boron isotopes in precipitation: experimental constraints and field evidence from French Guiana. *Earth Planet. Sci. Lett.* **235**, 16–30.

Craig, H., 1961. Isotopic variations in meteoric waters. *Science* **133**, 1702–1703.

Craig, H., Gordon, L., 1965. Deuterium and oxygen 18 variations in the ocean and marine atmosphere. In: Tongiorgi, E. (Ed.), *Stable Isotopes in Oceanographic Studies and Palaeotemperatures, Spoleto 1965*. Consiglio Nazionale della Richerche, Pisa, Italy, pp. 9–130.

Dansgaard, W., 1964. Stable isotopes in precipitation. *Tellus* **16**, 436–468.

Davidson, G.R., Bassett, R.L., 1993. Application of boron isotopes for identifying contaminants such as fly ash leachate in groundwater. *Environ. Sci. Technol.* **27**, 172–176.

Duce, R.A., 1996. Atmospheric biogeochemical cycles of selenium, arsenic and boron. In: Boutron, C.F. (Ed.), *Physics and chemistry of the atmospheres of the Earth and other objects of the solar system*, vol. 2. Les Editions de Physique, pp. 157–182.

Eisenhut, S., Heumann, K.G., 1997. Identification of groundwater contaminations by landfills using boron isotope measurements with negative thermal ionisation mass spectrometry. *Fresenius J. Analy. Chem.* **359**, 375–377.

Eriksson, E., 1957. The chemical composition of Hawaiian rainfall. *Tellus* **9**, 509–520.

Fogg, T.R., Duce, R.A., 1985. Boron in the troposphere: distribution and fluxes. *J. Geophys. Res.* **90** (D2), 3781–3796.

Friedman, I., O'Neil, J.R., 1977. Compilation of stable isotope fractionation factors of geochemical interest. U.S. Geol. Surv. Prof. Paper, 440-KK.

Galy, A., 1999. Etude géochimique de l'érosion actuelle de la chaîne Himalayenne. Ph.D. Thesis, INPL, Nancy (France).

Galy, A., France-Lanord, C., Derry, L., 1999. The strontium isotopic budget of Himalayan Rivers in Nepal and Bangladesh. *Geochim. Cosmochim. Acta* **63** (13/14), 1905–1925.

Hemming, N.G., Hanson, G.N., 1992. Boron isotopic composition and concentration in modern marine carbonates. *Geochim. Cosmochim. Acta* **56**, 537–543.

IAEA/WMO, 2004. Global Network of Isotopes in Precipitation. The GNIP Database (GNIP2001monthly). Accessible at: http://isohis.iaea.org.

Junge, C.E., 1963. *Air chemistry and radioactivity*. Academic Press, New York, pp. 1–382.

Kakihana, H., Kotaka, M., Satoh, S., Nomura, M., Okamoto, M., 1977. Fundamental studies on the ion-exchange separation of boron isotopes. *Bull. Chem. Soc. Japan* **50** (1), 158–163.

Kanzaki, T., Yoshida, M., Nomura, M., Kakihana, H., Ozawa, T., 1979. Boron isotopic composition of fumarolic condensates and sassolites from Satsuma Iwo-jima, Japan. *Geochim. Cosmochim. Acta* **43** (11), 1859–1863.

Kotaka, M., 1973. Chromatographic separation of boron and nitrogen isotopes using pure water as eluent. PhD dissertation, Tokyo Institute of Technology.

Leeman, W.P., Vocke, R.D., McKibben, M.A., 1992. Boron isotopic fractionation between coexisting vapor and liquid in natural geothermal systems. In: Kharaka, Y.K., Maest, A.S. (Eds.), *7th WRI, Utah, USA*. A A Balkema, Rotterdam, pp. 1007–1010.

Lemarchand, D., Gaillardet, J., Levin, E., Allègre, C.J., 2000. The influence of rivers on marine boron isotopes and implications for reconstructing past ocean pH. *Nature* **408**, 951–954.

Michard, G., 1989. Equilibres chimiques dans les eaux naturelles. Editions Publisud.

Miyata, Y., Tokieda, T., Amakawa, H., Uematsu, M., Nozaki, Y., 2000. Boron isotope variations in the atmosphere. *Tellus* **52B** (4), 1057–1065.

Négrel, P., Lachassagne, P., Laporte, P., 1997. Caractérisation chimique et isotopique des pluies de Cayenne (Guyane Française). *Comptes rendus de l'Académie des Sciences—sér. 2—Sciences de la Terre et des Planètes* **324**, 379–386.

Nomura, M., Kanzaki, T., Ozawa, T., Okamoto, M., Kakihana, H., 1982. Boron isotopic composition of fumarolic condensates from some volcanoes in Japanese island arcs. *Geochim. Cosmochim. Acta* **46**, 2403–2406.

Palmer, M.R., Spivack, A.J., Edmond, J.M., 1987. Temperature and pH controls over isotopic fractionation during adsorption of boron on marine clay. *Geochim. Cosmochim. Acta* **51**, 2319–2323.

Palmer, M.R., Sturchio, N.C., 1990. The boron isotope systematics of the Yellowstone National Park (Wyoming) hydrothermal system: A reconnaissance. *Geochim. Cosmochim. Acta* **54** (10), 2811–2815.

Palmer, M.R., Swihart, G.H., 1996. Boron isotope geochemistry: an overview. In: Grew, E.S., Anovitz, L.M. (Eds.), Boron, Mineralogy, Petrology and Geochemistry. vol. 33, Reviews in Mineralogy, pp. 709–744.

Rose, E., 1999. Géochimie isotopique du bore dans les cycles supergènes, Ph.D. Thesis, Institut National Polytechnique de Lorraine, 201.

Rose, E.F., Carignan, J., Chaussidon, M., 2000a. Transfer of atmospheric Boron from oceans to continents: An investigation using precipitation waters and epiphytic lichens. Geochem. Geophys. Geosyst. 1 (2000GC000077).

Rose, E.F., Chaussidon, M., France-Lanord, C., 2000b. Fractionation of boron isotopes during erosion processes: the example of Himalayan rivers. *Geochim. Cosmochim. Acta* **64** (3), 397–408.

Rose, E.F., Shimizu, N., Layne, G.D., Grove, T.L., 2001. Melt beneath Mt. Shasta from boron data in primitive melt inclusions. *Science* **293**, 281–283.

Rozanski, K., Araguas-Araguas, L., Gonfiantini, R., 1993. Isotopic patterns in modern global precipitation. In: Climate Change in Continental Isotopic Records, vol. 78, American Geophysical Union. pp. 1–36.

Schwarcz, H.P., Agyei, E.K., McMullen, C.C., 1969. Boron isotopic fractionation during clay adsorption from sea-water. *Earth Planet. Sci. Lett.* **6**, 1–5.

Simonetti, A., Gariépy, C., Carignan, J., 2000a. Pb and Sr isotopic compositions of snowpack from Québec, Canada: inferences on the sources and deposition budgets of atmospheric heavy metals. *Geochim. Cosmochim. Acta* **64** (1), 5–20.

Simonetti, A., Gariépy, C., Carignan, J., Poissant, L., 2000b. Isotopic evidence of trace metal sources and transport in eastern Canada as recorded from wet deposition. *J. Geophys. Res.-Atmos.* **105** (D10), 12263–12278.

Spivack, A.J., 1986. Boron isotope geochemistry. Ph.D. Thesis, M.I.T., Woods Hole Oceanographic Institution.

Spivack, A.J., Edmond, J.M., 1987. Boron isotope exchange between seawater and the oceanic crust. *Geochim. Cosmochim. Acta* **51**, 1033–1043.

Spivack, A.J., Berndt, M.E., Seyfried Jr, W.E., 1990. Boron isotope fractionation during supercritical phase separation. *Geochim. Cosmochim. Acta* **54**, 2337–2339.

Xiao, Y., Sun, D., Wang, Y., Qi, H., Jin, L., 1992. Boron isotopic compositions of brine, sediments, and source water in Da Qaidam Lake, Qinghai, China. *Geochim. Cosmochim. Acta* **56**, 1561–1568.

Xiao, Y., Swihart, G.H., Xiao, Y., Vocke Jr, R.D., 2001. A preliminary experimental study of the boron concentration in vapor and the isotopic fractionation of boron between seawater and vapor during evaporation of seawater. *Sci. China Ser. B* **44** (5), 540–551.

Zhao, Z., Liu, C., Xiao, Y., Lang, Y., 2003. Geochemical study of boron isotopes in the process of loess weathering. *Sci. China Ser. D* **46** (2), 106–116.